Chemistry of Polynuclear Metal Complexes with Bridging Carbene or Carbyne Ligands. Part 101.[1] Synthesis of the Compounds $[\mathrm{WPt}(\mu\text{-}\mathrm{CC_6H_4Me\text{-}4})(\mu\text{-}\sigma{:}\eta^x\text{-}\mathrm{C_2B_nH_{n-1}Me_2})(\mathrm{CO})_2(\mathrm{PMe_2Ph})_2]$ ($x = 5, n = 9$; $x = 6, n = 10$); Crystal Structures of an Isomer of Each Complex *

Nicholas Carr, M. Concepción Gimeno, and F. Gordon A. Stone
Department of Inorganic Chemistry, The University, Bristol BS8 1TS

In acetone at ambient temperatures, the reagents $[\mathrm{PtCl(Me)(PMe_2Ph)_2}]$, $\mathrm{TlBF_4}$, and $[\mathrm{NEt_4}][\mathrm{W}(\equiv\mathrm{CC_6H_4Me\text{-}4})(\mathrm{CO})_2(\eta^5\text{-}\mathrm{C_2B_9H_9Me_2})]$ afforded $[\mathrm{WPt}(\mu\text{-}\mathrm{CC_6H_4Me\text{-}4})(\mu\text{-}\sigma{:}\eta^5\text{-}\mathrm{C_2B_9H_8Me_2})(\mathrm{CO})_2(\mathrm{PMe_2Ph})_2]$ (two isomers), and a small amount of a salt formulated as $[\mathrm{PtMe(PMe_2Ph)_3}][\mathrm{W_2Pt}(\mu\text{-}\mathrm{CC_6H_4Me\text{-}4})_2(\mu\text{-}\sigma{:}\eta^5\text{-}\mathrm{C_2B_9H_8Me_2})(\mathrm{CO})_4(\eta^5\text{-}\mathrm{C_2B_9H_9Me_2})]$. The structure of one isomer of the dimetal compound was determined by *X*-ray diffraction. The W–Pt bond [2.720(1) Å] is spanned by the *p*-tolylmethylidyne group [W–μ-C 1.89(1), Pt–μ-C 2.14(1) Å] and by a $\mathrm{C_2B_9}$ fragment. The latter is co-ordinated to the W atom *via* the open pentagonal face of the *nido*-icosahedral cage, and bridges to the Pt atom through an exopolyhedral B–Pt σ bond [2.17(1) Å]. This boron atom is in the β site with respect to the carbon atoms in the $\overline{\mathrm{B}\mathit{B}\mathrm{BCC}}$ ring. In the other isomer it is the boron α to a carbon atom which forms the B–Pt bond. The reaction between the compounds $[\mathrm{PtCl(Me)(PMe_2Ph)_2}]$, $\mathrm{TlBF_4}$, and $[\mathrm{NEt_4}][\mathrm{W}(\equiv\mathrm{CC_6H_4Me\text{-}4})(\mathrm{CO})_2(\eta^6\text{-}\mathrm{C_2B_{10}H_{10}Me_2})]$ in thf (tetrahydrofuran) also yields two isomers of a dimetal species $[\mathrm{WPt}(\mu\text{-}\mathrm{CC_6H_4Me\text{-}4})(\mu\text{-}\sigma{:}\eta^6\text{-}\mathrm{C_2B_{10}H_9Me_2})(\mathrm{CO})_2(\mathrm{PMe_2Ph})_2]$. The structure of the isomer formed in greatest yield (*ca.* 70%) was established by *X*-ray diffraction. The W–Pt bond [2.738(1) Å] is bridged by the alkylidyne group [W–μ-C 1.92(1), Pt–μ-C 2.14(1) Å] and by a $\mathrm{C_2B_{10}}$ fragment. The non-planar $\overline{\mathrm{CBCBBB}}$ face of the latter is η^6 co-ordinated to the tungsten, but the cage also forms a B–Pt σ bond [2.15(1) Å]. This linkage involves a boron atom of the $\mathrm{B_3}$ group α to a carbon, and correspondingly the other isomer is assigned a structure in which it is the $\overline{\mathrm{CBCB}\mathit{B}\mathrm{B}}$ atom of the hexagonal ring which bonds to platinum. The n.m.r. data (^{1}H, ^{13}C-{^{1}H}, ^{11}B-{^{1}H}, and ^{31}P-{^{1}H}) for the new compounds are reported, and are in agreement with the structures proposed.

We have previously reported[2] reactions between the hydridoplatinum complex $[\mathrm{PtH(Me_2CO)(PEt_3)_2}][\mathrm{BF_4}]$ and the salts $[\mathrm{X}][\mathrm{W}(\equiv\mathrm{CR})(\mathrm{CO})_2(\eta^5\text{-}\mathrm{C_2B_9H_9Me_2})]$ [(**1a**), X = $\mathrm{N(PPh_3)_2}$, R = $\mathrm{C_6H_4Me\text{-}4}$; (**1b**), X = $\mathrm{NEt_4}$, R = $\mathrm{C_6H_3Me_2\text{-}2,6}$]. The products obtained have unusual structures. Thus (**1a**) and the platinum reagent afford the dimetal compound $[\mathrm{WPt(CO)_2(PEt_3)_2}\{\eta^6\text{-}\mathrm{C_2B_9H_8(CH_2C_6H_4Me\text{-}4)Me_2}\}]$ (**2**) in which the tungsten atom is ligated by a novel $\eta^6\text{-}\mathrm{C_2B_9H_8(CH_2C_6H_4Me\text{-}4)Me_2}$ group. Six atoms, $\overline{\mathrm{BCBBBC}}$, in the face of the ligand are co-ordinated to the metal, but the C ⋯ C separation within the hexahapto ring is non-bonding.[2a] Treatment of (**2**) with $\mathrm{PMe_3}$ or CO yields the complexes $[\mathrm{WPt}(\mu\text{-H})\{\mu\text{-}\sigma{:}\eta^5\text{-}\mathrm{C_2B_9H_7(CH_2C_6H_4Me\text{-}4)Me_2}\}(\mathrm{CO})_2\mathrm{L(PEt_3)_2}]$ [L = $\mathrm{PMe_3}$, (**3a**); or CO, (**3b**)]. These compounds contain exopolyhedral B–Pt σ bonds, but the $\mathrm{C_2B_9}$ fragments now ligate the tungsten in the customary η^5 manner. Thus formation of compound (**2**) from (**1a**) involves transformation of a *closo* icosahedral carbametallaborane framework into a *hyper-closo* structure. Subsequent addition of an electron-pair donor molecule to the former species results in the reformation of a *closo* $\mathrm{C_2B_9W}$ cage in the complexes (**3**).

The reaction between the salt (**1b**) and the hydridoplatinum compound follows a different pattern.[2b] The product initially isolated is the complex $[\mathrm{WPtH}(\mu\text{-}\mathrm{CC_6H_3Me_2\text{-}2,6})(\mathrm{CO})_2(\mathrm{PEt_3})(\eta^5\text{-}\mathrm{C_2B_9H_9Me_2})]$ (**4**) having an exopolyhedral three-centre two-electron B–H⇀Pt bond. Compound (**4**) readily releases molecular hydrogen to afford $[\mathrm{WPt}(\mu\text{-}\mathrm{CC_6H_3Me_2\text{-}2,6})(\mu\text{-}\sigma{:}\eta^5\text{-}\mathrm{C_2B_9H_8Me_2})(\mathrm{CO})_2(\mathrm{PEt_3})]$ (**5**).

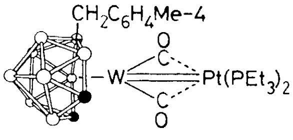

(**2**)

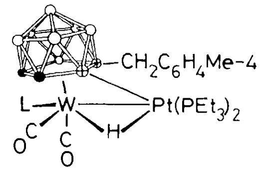

	L
(**3a**)	$\mathrm{PMe_3}$
(**3b**)	CO

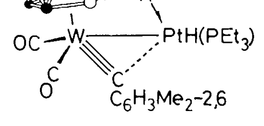

(**4**)

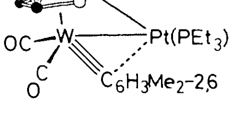

(**5**)

● CMe ○ BH ⊕ B

An *X*-ray diffraction study on the latter species established that the exopolyhedral B–Pt σ bond is formed by the central boron of the $\overline{\mathrm{B}\mathit{B}\mathrm{BCC}}$ ring ligating the tungsten, *i.e.* the boron atom which is in the β rather than in the α position with respect to the

---

* *Supplementary data available:* see Instructions for Authors, *J. Chem. Soc., Dalton Trans.*, 1990, Issue 1, pp. xix—xxii.

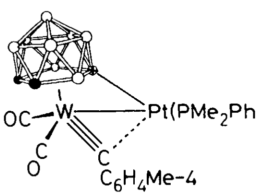

β isomer

(**7a**)

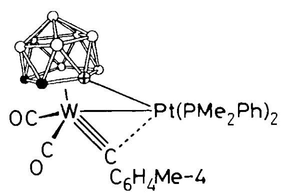

α isomer

(**7b**)

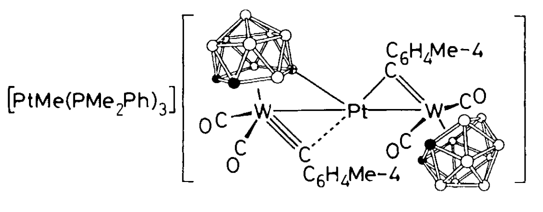

(**8**)

● CMe ○ BH ⊕ B

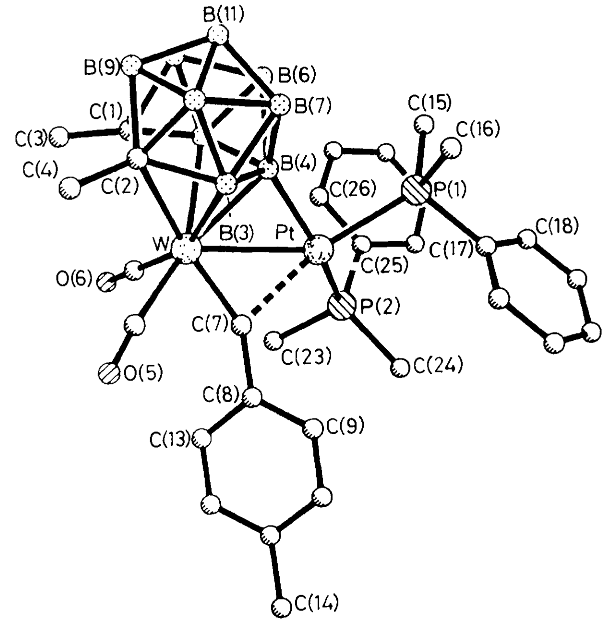

Figure 1. Molecular structure of $[\mathrm{WPt(\mu\text{-}CC_6H_4Me\text{-}4)(\mu\text{-}\sigma{:}\eta^5\text{-}C_2B_9H_8Me_2)(CO)_2(PMe_2Ph)_2}]$ (**7a**), showing the atom labelling scheme

two carbons. However, spectroscopic studies[2b] showed that the synthesis of (**5**) was accompanied by production of a small amount (*ca.* 5%) of an isomer in which it is a boron atom α to a carbon in the face of the cage which forms the B–Pt σ bond. It is likely that this species is derived from an isomer of (**4**) having a corresponding structure, with the B–H→Pt linkage also employing a boron atom adjacent to a carbon. However, no spectroscopic evidence for such an isomer was obtained. The existence of α or β isomers for these structures is relevant to the new work reported herein.

It has been previously shown[3] that treatment of the complex $[\mathrm{PtCl(Me)(PMe_2Ph)_2}]$ with electron-pair donor molecules (L) in polar solvents, and in the presence of $\mathrm{PF_6}^-$, affords the salts $[\mathrm{PtMe(L)(PMe_2Ph)_2}][\mathrm{PF_6}]$. We have employed this method to prepare $[\mathrm{PtMe(Me_2CO)(PMe_2Ph)_2}][\mathrm{BF_4}]$ *in situ*, and have investigated the reaction of this species with $[\mathrm{NEt_4}][\mathrm{W(\equiv CC_6H_4Me\text{-}4)(CO)_2(\eta^5\text{-}C_2B_9H_9Me_2)}]$ (**1c**). The motive for this study was to compare the nature of any products obtained with compound (**2**), isolated previously using the reagents (**1a**) and $[\mathrm{PtH(Me_2CO)(PEt_3)_2}][\mathrm{BF_4}]$.[2a] We have also investigated the reaction between the compounds $[\mathrm{PtMe(thf)(PMe_2Ph)_2}][\mathrm{BF_4}]$ (thf = tetrahydrofuran) and $[\mathrm{NEt_4}][\mathrm{W(\equiv CC_6H_4Me\text{-}4)(CO)_2(\eta^6\text{-}C_2B_{10}H_{10}Me_2)}]$ (**6**).

Results and Discussion

A mixture of the compounds $[\mathrm{PtCl(Me)(PMe_2Ph)_2}]$, $\mathrm{TlBF_4}$, and (**1c**), in acetone at room temperature, affords the compounds $[\mathrm{WPt(\mu\text{-}CC_6H_4Me\text{-}4)(\mu\text{-}\sigma{:}\eta^5\text{-}C_2B_9H_8Me_2)(CO)_2(PMe_2Ph)_2}]$ [two isomers, (**7a**) and (**7b**)] and $[\mathrm{PtMe(PMe_2Ph)_3}][\mathrm{W_2Pt(\mu\text{-}CC_6H_4Me\text{-}4)_2(\mu\text{-}\sigma{:}\eta^5\text{-}C_2B_9H_8Me_2)(CO)_4(\eta^5\text{-}C_2B_9H_9Me_2)}]$ (**8**). The two isomers (**7a**) and (**7b**), and compound (**8**), are separable by column chromatography. The salt (**8**) is only a minor product (*ca.* 5%). Its formulation is based on spectroscopic evidence only, as discussed later.

The isomers (**7a**) and (**7b**) were obtained as crystals in *ca.* 25 and 45% yield, respectively, and hence these complexes could be fully characterised by microanalysis, and by n.m.r. studies (Tables 1 and 2). Moreover, the structure of (**7a**) was established by a single-crystal *X*-ray diffraction study. Discussion of the spectroscopic data is deferred until the results of the latter are described (see Table 3, and Figure 1).

The W–Pt bond is bridged by the *p*-tolylmethylidyne group and by the $\mathrm{C_2B_9H_8Me_2}$ fragment, the latter being η^5-co-ordinated to the tungsten and forming an exopolyhedral B–Pt bond [2.17(1) Å]. The atom [B(4)] forming this linkage is the unique boron in the $\overline{\mathrm{B}\mathit{B}\mathrm{BCC}}$ pentagonal face of the cage, being in the β position with respect to the carbon atoms. This feature of the structure is similar to that previously found in complex (**5**) [B–Pt 2.01(2) Å].[2b] As mentioned above, formation of (**5**) results from elimination of $\mathrm{H_2}$ from (**4**), and it is likely, therefore, that (**7a**) forms *via* a similar pathway involving a precursor having a B–H→Pt bridge bond. Such an intermediate could be formed by complexation of the C≡W bond in the anion of (**1c**) with a $[\mathrm{PtMe(PMe_2Ph)_2}]^+$ fragment derived from the labile species $[\mathrm{PtMe(Me_2CO)(PMe_2Ph)_2}]^+$. The presence in such a structure of a Pt–Me bond *cis* to a B–H→Pt linkage could lead to release of $\mathrm{CH_4}$ and formation of (**7a**), in a manner analogous to the loss of $\mathrm{H_2}$ from (**4**) to yield (**5**).

The tungsten atom in compound (**7a**) carries two terminally bound CO groups, and as expected the platinum the two $\mathrm{PMe_2Ph}$ ligands. The alkylidyne moiety asymmetrically bridges the metal–metal bond [W–C(7) 1.89(1) and Pt–C(7) 2.14(1) Å]. These distances are essentially the same as those found in (**5**) [W–μ-C 1.88(1) and Pt–μ-C 2.15(1) Å]. Moreover, the W–μ-C separations in both compounds are very similar to those for the C≡W distances in the compounds $[\mathrm{W(\equiv CC_6H_4Me\text{-}4)(CO)_2(\eta\text{-}C_5H_5)}]$ [1.82(2) Å][4] and $[\mathrm{PPh_4}][\mathrm{W(\equiv CC_6H_4Me\text{-}4)(CO)_2(\eta^5\text{-}C_2B_9H_9Me_2)}]$ [1.83(1) Å].[5] In complexes in which tungsten is bonded to another transition element and where there is a bridging *p*-tolylmethylidyne group the W–μ-C distances are generally longer (*ca.* 1.91—2.03 Å)[6] than those found in (**5**) or (**7a**). An opposite trend is shown in the Pt–μ-C separations. The Pt–C(7) distance in (**7a**) is perceptibly longer than that in $[\mathrm{WPt(\mu\text{-}CC_6H_4Me\text{-}4)(CO)_2(PMe_2Ph)_2(\eta\text{-}C_5H_5)}]$ [2.00(1) Å].[7] It is interesting to compare also the W–μ-C–C′(aryl) angles in the different species. For (**5**)[2b] and (**7a**) these are 175(1) and 151(1)°, respectively, while for $[\mathrm{WPt(\mu\text{-}CC_6H_4Me\text{-}4)(CO)_2(PMe_2Ph)_2(\eta\text{-}C_5H_5)}]$ the angle is 138(1)°, and is thus appreciably smaller. These data suggest that attachment of the $\mathrm{Pt(PMe_2Ph)_2}$ fragment to the C≡W groups in the three compounds causes the least perturbation of the carbon–tungsten triple bond in (**5**) and the most in $[\mathrm{WPt(\mu\text{-}CC_6H_4Me\text{-}4)(CO)_2(PMe_2Ph)_2(\eta\text{-}C_5H_5)}]$, with (**7a**) displaying behaviour intermediate between the two.

Table 1. Hydrogen-1 and carbon-13 n.m.r. data[a] for the tungsten–platinum complexes

Compound	^{1}H(δ)	^{13}C[b](δ)
(7a)	0.85 [d, 6 H, MeP, J(PH) 8, J(PtH) 20], 1.51 [d, 6 H, MeP, J(PH) 11, J(PtH) 18], 2.18 (s, 6 H, CMe), 2.35 (s, 3 H, Me-4), 7.14—7.38 (m, 14 H, C_6H_4 and Ph)	[c] 290.4 [d, μ-C, J(PC) 36], 223.5 [CO, J(WC) 171], 153.8—123.7 (C_6H_4 and Ph), 60.6 (*C*Me), 30.4 (C*Me*), 21.5 (Me-4), 16.8 [d, MeP, J(PC) 41, J(PtC) 60], 13.9 [d, MeP, J(PC) 24]
(7b)	0.58 [d, 3 H, MeP, J(PH) 8, J(PtH) 16], 1.05 [d, 3 H, MeP, J(PH) 9, J(PtH) 18], 1.40 [d, 3 H, MeP, J(PH) 11, J(PtH) 41], 1.75 [d, 3 H, MeP, J(PH) 11, J(PtH) 34], 1.99, 2.32, 2.57 (s × 3, 9 H, CMe and Me-4), 6.94—7.37 (m, 14 H, C_6H_4 and Ph)	284.1 [d, μ-C, J(PC) 34], 226.1, 222.8 (CO), 154.1—128.2 (C_6H_4 and Ph), 63.2, 59.1 (*C*Me), 35.9, 29.3 (C*Me*), 21.5 (Me-4), 19.4 [d, MeP, J(PC) 44, J(PtC) 54], 14.8 [d, MeP, J(PC) 29, J(PtC) 22], 14.5 [d, MeP, J(PC) 27, J(PtC) 54], 12.2 [d, MeP, J(PC) 22]
(8)	[c] 0.48 [d of t, 3 H, MePt, J(PH) 8 and 6, J(PtH) 57], 1.12 [d, 6 H, MeP, J(PH) 8, J(PtH) 18], 1.55 [t, 12 H, MeP, J(PH)[d] 7, J(PtH) 30], 1.85, 1.94, 2.13, 2.14, 2.15, 2.18 (s × 6, 18 H, CMe and Me-4), 6.94—7.50 (m, 23 H, C_6H_4 and Ph)	311.1, 293.2 (μ-C), 227.1, 221.6, 221.1, 220.6 (CO), 152.1—127.5 (C_6H_4 and Ph), 72.2, 69.9, 68.0, 66.3 (*C*Me), 30.3, 30.0 (C*Me*), 21.6, 21.5 (Me-4), 16.5 [d, MeP, J(PC) 29], 14.1 [t, MeP, J(PC)[e] 36], 0.4 [d, MePt, J(PC) 76, J(PtC) 458]
(10a)	0.77 [d, 6 H, MeP, J(PH) 10, J(PtH) 20], 1.74 [d, 6 H, MeP, J(PH) 10, J(PtH) 37], 2.11 (s br, 6 H, CMe), 2.38 (s, 3 H, Me-4), 6.99—7.35 (m, 14 H, C_6H_4 and Ph)	296.9 [d, μ-C, J(PC) 44], 208.4 (CO), 154.1—127.9 (C_6H_4 and Ph), 72.5 (br, *C*Me), 34.5 (C*Me*), 21.0 (Me-4), 15.9 [d, MeP, J(PC) 39], 13.5 [d, MeP, J(PC) 27]
(10b)	0.59 [d, 3 H, MeP, J(PH) 8, J(PtH) 20], 0.93 [d, 3 H, MeP, J(PH) 9, J(PtH) 20], 1.45 [d, 3 H, MeP, J(PH) 11, J(PtH) 25], 1.78 [d, 3 H, MeP, J(PH) 11, J(PtH) 41], 1.69, 2.29, 2.50 (s × 3, 9 H, CMe and Me-4), 7.08—7.38 (m, 14 H, C_6H_4 and Ph)	276.6 [d, μ-C, J(PC) 48], 211.1, 205.5 (CO), 153.0—128.1 (C_6H_4 and Ph), 77.8, 74.9 (*C*Me), 40.5, 34.9 (C*Me*), 21.3 (Me-4), 18.3 [d, MeP, J(PC) 39], 15.5 [d, MeP, J(PC) 30], 14.4 [d, MeP, J(PC) 36], 11.7 [d, MeP, J(PC) 21]

[a] Chemical shifts are in p.p.m., coupling constants in Hz, measurements in CD_2Cl_2 at ambient temperatures, unless otherwise stated. [b] Hydrogen-1 decoupled, chemical shifts are positive to high frequency of $SiMe_4$. [c] Measured in $CDCl_3$. [d] $|^2J(PH) + {}^4J(PH)|$. [e] $|^1J(PC) + {}^3J(PC)|$.

Table 2. Boron-11 and phosphorus-31 n.m.r. data[a] for the tungsten–platinum compounds

Compound	^{11}B(δ)[b]	^{31}P(δ)[c]
(7a)	[d] 48.2 [d, 1 B, J(PB) 68, J(PtB) 533] −7.8 to −26.8 (br, 8 B)	[e] −2.3 [d, J(PP) 25, J(PtP) 3 607] −5.2 [vbr, J(PtP) *ca.* 2 500]
(7b)	38.3 [d, 1 B, J(PB) 73, J(PtB) 580] 0.2 to −18.4 (br, 8 B)	[e] −5.6 [vbr, J(PtP) *ca.* 2 100] −7.3 [d, J(PP) 25, J(PtP) 3 442]
(8)[f]	38.5 [br, 1 B, J(PtB) 732] −5.9 to −16.9 (br, 17 B)	−5.8 [d, J(PP) 24, J(PtP) 2 672] −13.1 [t, J(PP) 24, J(PtP) 1 827]
(10a)	54.5 [br, 1 B, J(PtB) 450] −1.7 to −21.6 (br, 9 B)	−4.9 [d, J (PP) 26, J(PtP) 3 345] −7.3 [br, J(PtP) *ca.* 2 600]
(10b)	47.2 [d, 1 B, J(PB) 61, J(PtB) 452] 10.3 to −29.9 (br, 9 B)	−7.0 [d, J(PP) 26, J(PtP) 3 483] −10.0 [br, J(PtP) *ca.* 2 500]

[a] Chemical shifts in p.p.m., coupling constants in Hz, measurements in CD_2Cl_2 at ambient temperatures unless otherwise stated. [b] Hydrogen-1 decoupled, chemical shifts are positive to high frequency of $BF_3 \cdot Et_2O$ (external). [c] Hydrogen-1 decoupled, chemical shifts are positive to high frequency of 85% H_3PO_4 (external). [d] Measured in $CDCl_3$. [e] Measured in $(CD_3)_2CO$. [f] ^{195}Pt-{^{1}H} N.m.r. (in $CDCl_3$): δ −25 (WPtW) and −387 p.p.m. [d of t, PtP_3, J(PtP) 2 672 and 1 827 Hz]; chemical shifts are to high frequency of $\Xi(^{195}Pt) = 21.4$ MHz.

The W–Pt bond in **(7a)** [2.720(1) Å] is very similar in length to that in **(5)** [2.728(1) Å]. In [WPt(μ-CC_6H_4Me-4)$(CO)_2$$(PMe_2Ph)_2$(η-$C_5H_5$)] the metal–metal bond is 2.751(1) Å. These distances may be compared with those in compounds **(3a)** [2.843(2) Å] and **(2)** [2.602(1) Å].[2a] However, the latter linkage is thought to correspond to a W=Pt bond.

In compound **(7a)** two tertiary phosphine groups ligate the platinum atom. This is in contrast with **(5)** which contains only one such group. Treatment of the latter with 1 equivalent of a tertiary phosphine leads only to decomposition, and not a product containing a $Pt(PR_3)_2$ group (R = alkyl or aryl). Presumably the bulky μ-$CC_6H_3Me_2$-2,6 fragment prevents the formation of a stable compound containing a $Pt(PR_3)_2$ moiety. In contrast, the rod-like ligands CO or CNBu^t add to **(5)** to yield the complexes [WPt(μ-$CC_6H_3Me_2$-2,6)(μ-σ:η^5-$C_2B_9H_8$-Me_2)(PEt_3)L] [L = CO, **(9a)** or CNBu^t, **(9b)**].[2b]

Having established the structure of **(7a)**, the spectroscopic data are readily interpretable. The i.r. spectrum displays two CO stretching bands (1 976 and 1 902 cm^{-1}). The presence of the B(4)–Pt bond is revealed in the ^{11}B-{^{1}H} n.m.r. spectrum (Table 2) by a doublet resonance at δ 48.2 p.p.m. [J(PB) 68 Hz], with ^{195}Pt satellite peaks [J(PtB) 533 Hz]. This spectrum is very similar to that of complex **(9a)** in which the signal for the BPt group occurs at δ 47.0 p.p.m., with J(PtB) 508 Hz. The ^{31}P-{^{1}H} n.m.r. spectrum of **(7a)** displays a doublet resonance at δ −2.3 p.p.m. [J(PP) 25 Hz] and a broad peak at δ −5.2 p.p.m. The latter may be ascribed to the P(2) nucleus transoid to B(4) [B(4)–Pt–P(2) 154.1(4)°], the broadening of the signal being due to unresolved ^{11}B–^{31}P and ^{31}P–^{31}P coupling.

The ^{13}C-{^{1}H} n.m.r. spectrum shows a doublet resonance for the μ-C nucleus at δ 290.4 p.p.m. [J(PC) 36 Hz]. The chemical shift is indicative of the semibridging nature of this atom, as

Table 3. Selected internuclear distances (Å) and angles (°) for $[WPt(\mu\text{-}CC_6H_4Me\text{-}4)(\mu\text{-}\sigma{:}\eta^5\text{-}C_2B_9H_8Me_2)(CO)_2(PMe_2Ph)_2]$ (**7a**)

W–Pt	2.720(1)	Pt–P(1)	2.271(4)	Pt–P(2)	2.366(4)	W–C(1)	2.52(1)
W–C(2)	2.48(1)	W–B(3)	2.35(2)	W–B(4)	2.21(2)	Pt–B(4)	2.17(1)
W–B(5)	2.37(2)	W–C(5)	2.00(2)	W–C(6)	1.98(2)	W–C(7)	1.89(1)
Pt–C(7)	2.14(1)	C(1)–C(2)	1.61(2)	C(1)–C(3)	1.55(2)	C(1)–B(5)	1.66(3)
C(1)–B(9)	1.73(2)	C(1)–B(10)	1.71(2)	C(2)–C(4)	1.54(3)	C(2)–B(3)	1.72(2)
C(2)–B(8)	1.74(2)	C(2)–B(9)	1.73(2)	B(3)–B(4)	1.82(3)	B(3)–B(7)	1.77(2)
B(3)–B(8)	1.72(2)	B(4)–B(5)	1.78(2)	B(4)–B(6)	1.79(2)	B(4)–B(7)	1.82(2)
B(5)–B(6)	1.81(2)	B(5)–B(10)	1.75(2)	B(6)–B(7)	1.79(3)	B(6)–B(10)	1.75(3)
B(6)–B(11)	1.76(3)	B(7)–B(8)	1.76(3)	B(7)–B(11)	1.75(2)	B(8)–B(9)	1.75(2)
B(8)–B(11)	1.74(3)	B(9)–B(10)	1.73(3)	B(9)–B(11)	1.70(3)	B(10)–B(11)	1.76(3)
C(5)–O(5)	1.15(2)	C(6)–O(6)	1.17(2)	C(7)–C(8)	1.46(2)		
W–Pt–P(1)	142.1(1)	W–Pt–P(2)	120.1(1)	W–C(5)–O(5)	174(1)	W–C(6)–O(6)	178(2)
C(5)–W–C(6)	90(1)	W–C(7)–C(8)	151(1)	Pt–C(7)–C(8)	124(1)	Pt–W–C(7)	51.6(4)
W–Pt–C(7)	43.9(3)	P(1)–Pt–C(7)	162.1(3)	P(2)–Pt–C(7)	89.0(4)	P(1)–Pt–P(2)	95.0(1)
P(1)–Pt–B(4)	89.8(4)	P(2)–Pt–B(4)	154.1(4)	C(1)–B(5)–B(4)	106(1)	B(3)–B(4)–B(5)	106(1)
C(2)–B(3)–B(4)	104(1)	C(1)–C(2)–B(3)	111(1)	C(2)–C(1)–B(5)	113(1)		

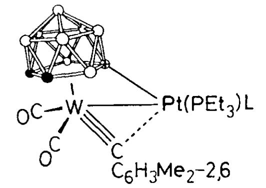

L

(**9a**) CO

(**9b**) CNBu^t

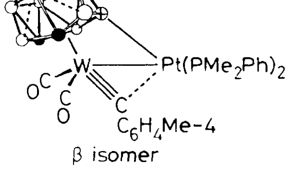

β isomer

(**10a**)

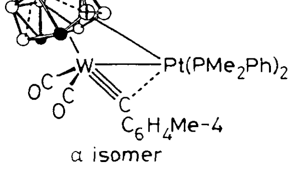

α isomer

(**10b**)

● CMe ○ BH ⊕ B

discussed previously.[1,2b] Correspondingly, in the spectrum of the structurally related complex (**9a**) the μ-C resonance is at δ 287.9 p.p.m. [*J*(PC) 29 Hz].[2b] In contrast with (**7a**) or (**9a**), in the $^{13}C\text{-}\{^1H\}$ n.m.r. spectrum of the compound $[WPt(\mu\text{-}CC_6H_4\text{-}Me\text{-}4)(CO)_2(PMe_2Ph)_2(\eta\text{-}C_5H_5)]$ the resonance for the μ-C nucleus is at δ 336 p.p.m. [*J*(PC) 59 Hz].[7] The more deshielded signal and the larger $^{31}P\text{-}^{13}C$ coupling reflect the stronger μ-C–Pt bonding in this compound compared with (**7a**) or (**9a**). As a consequence of the B–Pt σ bond involving B(4), rather than the equivalent but less-symmetrical sites B(3) or B(5), the CMe groups are in similar environments. Hence in the $^{13}C\text{-}\{^1H\}$ n.m.r. spectrum only one *C*Me and one C*Me* resonance is observed. Correspondingly, there is only one CMe peak in the ^1H n.m.r. spectrum.

There are strong similarities between the n.m.r. data for the isomers (**7a**) and (**7b**), as would be expected. However, having established the structure of the former by *X*-ray diffraction, it became obvious from the ^1H and $^{13}C\text{-}\{^1H\}$ n.m.r. data that the latter had a less-symmetrical structure. This would be the situation if the B–Pt bond in (**7b**) involved a boron atom adjacent to a carbon in the face of the ligand co-ordinated to the tungsten. Thus the ^1H n.m.r. spectrum showed two CMe signals, and the $^{13}C\text{-}\{^1H\}$ n.m.r. spectrum had two *C*Me and two C*Me* resonances (Table 1). The $^{13}C\text{-}\{^1H\}$ n.m.r. spectrum also displayed two CO peaks, in contrast with that of (**7a**) which only showed one. The μ-C signal is a doublet [*J*(PC) 34 Hz] at δ 284.1 p.p.m. The signal for the BPt group in the $^{11}B\text{-}\{^1H\}$ n.m.r. spectrum is at δ 38.3 p.p.m., and as expected it is a doublet [*J*(PB) 73 Hz], with ^{195}Pt satellite peaks [*J*(PtB) 580 Hz] (Table 2). Thus (**7b**) can be designated as the α isomer, and could form *via* loss of CH_4 from an intermediate dimetal species having a B–H→Pt three-centre two-electron bond involving a boron next to carbon in the face of the cage.

As mentioned above, compound (**8**) was formed in very small amounts, and crystals for an *X*-ray diffraction study could not be obtained. Indeed, this product remained as an oil. There is good spectroscopic evidence, however, for its formulation as shown. The i.r. spectrum in the CO region showed four bands (see Experimental section), and there are also four CO resonances in the $^{13}C\text{-}\{^1H\}$ n.m.r. spectrum (Table 1). This spectrum also shows two distinct μ-C signals, that at δ 311.1 p.p.m. may be ascribed to a fully bridging $CC_6H_4Me\text{-}4$ fragment and that at δ 293.2 p.p.m. to a more asymmetrically bridging ligand.[2b,6,8] It was evident from the $^{11}B\text{-}\{^1H\}$ n.m.r. spectrum that one of the C_2B_9 cages formed a B–Pt bond and the other did not since there was a diagnostic resonance for the BPt group at δ 38.5 p.p.m. with ^{195}Pt satellite peaks [*J*(PtB) 732 Hz], and the other signals all broad corresponded to 17 boron nuclei.

The $^{195}Pt\text{-}\{^1H\}$ and $^{31}P\text{-}\{^1H\}$ n.m.r. spectra were informative since the data established the presence of a $[PtX(PR_3)_3]^+$ cation.[9] The $^{31}P\text{-}\{^1H\}$ spectrum consisted (Table 2) of a doublet at δ −5.8 p.p.m. [*J*(PP) 24 Hz], which may be assigned to the *trans* P–Pt–P group, and a triplet at δ −13.1 p.p.m. [*J*(PP) 24 Hz] due to the *trans*-P–Pt–X fragment. Both ^{31}P resonances show the expected $^{31}P\text{-}^{195}Pt$ couplings (1 827 and 2 672 Hz). In the $^{195}Pt\text{-}\{^1H\}$ n.m.r. spectrum the signal for the platinum atom in the $[PtMe(PMe_2Ph)_3]^+$ cation occurs at δ −387 p.p.m., with $^{31}P\text{-}^{195}Pt$ couplings of 1 827 and 2 672 Hz. The remaining ^{195}Pt resonance at −25 p.p.m. may be ascribed to a W–Pt–W group in which the metal–metal bonds are bridged by alkylidyne ligands. That X in the cation was a Me group was revealed from the ^1H n.m.r. spectrum by a resonance at δ 0.48, which appeared as a doublet of triplets [*J*(PH) 8 and 6 Hz], with ^{195}Pt satellites [*J*(PtH) 57 Hz]. In the $^{13}C\text{-}\{^1H\}$ n.m.r. spectrum a peak at δ 0.4 p.p.m. [*J*(PC) 76, *J*(PtC) 458 Hz] is also diagnostic for a MePt group on the basis of its chemical shift and the magnitude of the $^{195}Pt\text{-}^{13}C$ coupling.

The route by which the small quantities of compound (**8**) are produced is obscure. However, it is noteworthy that in the synthesis of complex (**4**) formation of the related cation

Table 4. Selected internuclear distances (Å) and angles (°) for the complex [WPt(μ-CC$_6$H$_4$Me-4)(μ-σ:η^6-C$_2$B$_{10}$H$_9$Me$_2$)(CO)$_2$(PMe$_2$Ph)$_2$] (**10b**)

W–Pt	2.738(1)	Pt–P(1)	2.284(3)	Pt–P(2)	2.362(3)	W–C(1)	2.31(1)
W–C(2)	2.38(1)	W–B(3)	2.41(2)	W–B(4)	2.23(1)	Pt–B(4)	2.15(1)
W–B(5)	2.42(1)	W–B(6)	2.55(2)	W–C(5)	2.02(1)	W–C(6)	2.01(2)
W–C(7)	1.92(1)	Pt–C(7)	2.14(1)	C(1)–C(3)	1.48(2)	C(1)–B(3)	1.58(2)
C(1)–B(6)	1.57(2)	C(1)–B(7)	1.84(2)	C(2)–C(4)	1.56(2)	C(2)–B(3)	1.72(2)
C(2)–B(4)	1.75(2)	C(2)–B(8)	1.63(2)	C(2)–B(9)	1.62(2)	B(3) ··· B(7)	2.05(2)
B(3)–B(8)	1.79(2)	B(4)–B(5)	1.79(2)	B(4)–B(9)	1.79(2)	B(4)–B(10)	1.79(2)
B(5)–B(6)	1.78(2)	B(5)–B(10)	1.77(2)	B(5)–B(11)	1.77(2)	B(6) ··· B(7)	2.00(2)
B(6)–B(11)	1.77(2)	B(7)–B(8)	1.88(2)	B(7)–B(11)	1.85(2)	B(7)–B(12)	1.79(2)
B(8)–B(9)	1.68(2)	B(8)–B(12)	1.73(2)	B(9)–B(10)	1.77(2)	B(9)–B(12)	1.79(2)
B(10)–B(11)	1.75(2)	B(10)–B(12)	1.77(2)	B(11)–B(12)	1.73(2)		
W–Pt–P(1)	139.4(1)	W–Pt–P(2)	121.4(1)	W–C(5)–O(5)	178(1)	W–C(6)–O(6)	175(1)
C(5)–W–C(6)	90(1)	W–C(7)–C(8)	149(1)	Pt–C(7)–C(8)	126(1)	Pt–W–C(7)	51.0(3)
W–Pt–C(7)	44.3(3)	P(1)–Pt–C(7)	168.2(2)	P(2)–Pt–C(7)	88.1(3)	P(1)–Pt–P(2)	94.8(1)
P(1)–Pt–B(4)	87.2(3)	P(2)–Pt–B(4)	161.5(3)	C(1)–B(3)–C(2)	121(1)	C(1)–B(6)–B(5)	120(1)
B(3)–C(1)–B(6)	122(1)	B(3)–C(2)–B(4)	119(1)	C(2)–B(4)–B(5)	116(1)	B(4)–B(5)–B(6)	116(1)

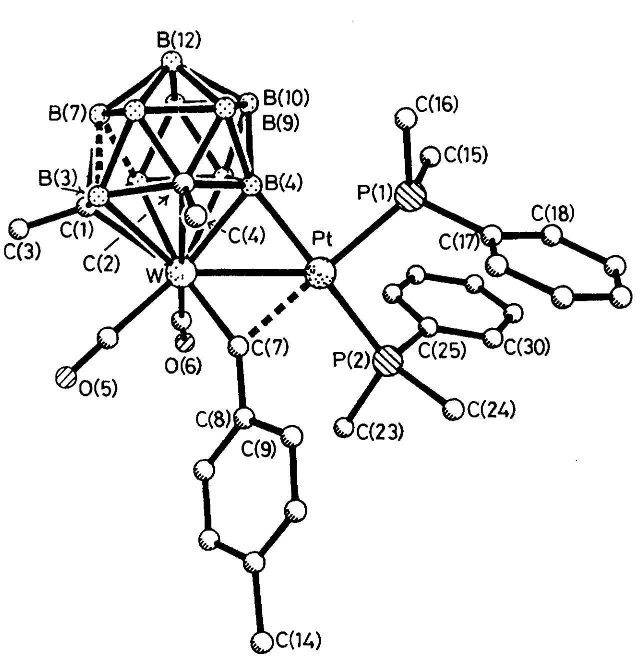

Figure 2. Molecular structure of [WPt(μ-CC$_6$H$_4$Me-4)(μ-σ:η^6-C$_2$B$_{10}$H$_9$Me$_2$)(CO)$_2$(PMe$_2$Ph)$_2$] (**10b**), showing the atom labelling scheme

[PtH(PEt$_3$)$_3$]$^+$ was observed as a by-product.[2b] This species is evidently produced by displacement of the acetone molecule in [PtH(Me$_2$CO)(PEt$_3$)$_2$][BF$_4$] by PEt$_3$, and a similar route involving PMe$_2$Ph and [PtMe(Me$_2$CO)(PMe$_2$Ph)$_2$][BF$_4$] would produce the cation of (**8**). The anion of this salt might form by displacement of the PMe$_2$Ph ligands in (**7a**) by a [MeC$_6$H$_4$C≡W(CO)$_2$(η^5-C$_2$B$_9$H$_9$Me$_2$)]$^-$ moiety. Earlier work has shown that the tertiary phosphine ligands of a Pt(PR$_3$)$_2$ group complexed by a C≡W system are labile.[10]

We have recently reported the salt [NEt$_4$][W(≡CC$_6$H$_4$Me-4)(CO)$_2$(η^6-C$_2$B$_{10}$H$_{10}$Me$_2$)] containing the 13-vertex WC$_2$B$_{10}$ group,[11] and it was of interest to study the reaction of this reagent with [PtCl(Me)(PMe$_2$Ph)$_2$] in the presence of TlBF$_4$. At room temperature, in thf (tetrahydrofuran) this combination of reactants afforded a mixture of two isomers of [WPt(μ-CC$_6$H$_4$Me-4)(μ-σ:η^6-C$_2$B$_{10}$H$_9$Me$_2$)(CO)$_2$(PMe$_2$Ph)$_2$] [(**10a**), β isomer; (**10b**), α isomer]. The isomers were readily separated by column chromatography on alumina, and it was observed that (**10b**) was formed in *ca.* 70% yield and (**10a**) in *ca.* 15% yield, the overall yield thus being high. The two compounds were characterised by microanalysis, and by n.m.r. spectroscopy (Tables 1 and 2). Suitable crystals of (**10b**) were grown for an *X*-ray crystallographic study, the results of which are summarised in Table 4, and the structure is shown in Figure 2.

The *X*-ray study established that in (**10b**), as in the complexes (**7**), there is a Pt–B σ bond, and that this linkage involves the boron atom [B(4)] adjacent to a carbon in the six-membered ring ligating the tungsten atom. Complex (**10b**) may for discussion purposes be described as the α isomer. The W–B(4) [2.23(1) Å] and Pt–B(4) [2.15(1) Å] distances in (**10b**) are essentially the same as those in compound (**7a**) (Table 3). The W–Pt bonds in the two species are also virtually the same [2.720(1) (**7a**) and 2.738(1) Å (**10b**)]. The Pt–μ-C separations in the two complexes are the same [2.14(1) Å], and the W–μ-C distances essentially so [1.89(1) (**7a**) and 1.92(1) Å (**10b**)]. In (**10b**), as in (**7a**), the W–C(7)–C(8) angle [149(1)°] is larger than the corresponding angle [138(1)°] in [WPt(μ-CC$_6$H$_4$Me-4)(CO)$_2$(PMe$_2$Ph)$_2$(η-C$_5$H$_5$)].[7] It thus seems appropriate to depict (**10b**) with a semibridging or asymmetric μ-CC$_6$H$_4$Me-4 group, as discussed for (**7a**) above.

The existence of the 13-vertex WC$_2$B$_{10}$ cage leads to different connectivities between the W atom and the ligating atoms of the cage, and also to distorted triangular faces within the carbaborane fragment.[11] These features result from the non-planar character of the $\overline{\text{CBCBBB}}$ face of the ligand. The linkages to the tungsten atom are: W–B(6) 2.55(2), W–B(5) 2.42(1), W–B(3) 2.41(2), W–C(2) 2.38(1), W–C(1) 2.31(1), and W–B(4) 2.23(1) Å. Additional distortions within the system probably result from the presence of the B(4)–Pt σ bond. The net result leads to B(3) and B(6) being in low connectivity sites with the B(3) ··· B(7) [2.05(2) Å] and B(6) ··· B(7) [2.00(2) Å] distances, represented by dotted lines in Figure 2, being appreciably longer than the other B–B separations. Consequently there are essentially two square faces about B(7). As far as we are aware, compound (**10b**) is only the second dimetal species known in which a C$_2$B$_{10}$ fragment bridges a metal–metal bond; the first reported species was [NEt$_4$][WFe(μ-CC$_6$H$_3$Me$_2$-2,6)(CO)$_4$(η^6-C$_2$B$_{10}$H$_{10}$-Me$_2$)] which contains a B–H→Pt bridge bond.[11]

Following the establishment of the structure of (**10b**), the spectroscopic data are readily interpreted. The B(4)Pt group reveals itself in the ^{11}B-{^{1}H} n.m.r. spectrum with a doublet resonance at δ 47.2 p.p.m. [*J*(PB) 61, *J*(PtB) 452 Hz]. The ^{31}P-{^{1}H} n.m.r. spectrum is as expected (Table 2), with two resonances for the non-equivalent PMe$_2$Ph ligands. As with (**7a**), the signal which is broad (δ −10.0 p.p.m.) can be assigned to the phosphorus nucleus P(2), transoid to B(4).

In the ^{13}C-{^{1}H} n.m.r. spectrum of (**10b**) (Table 1) the μ-C resonance is a doublet at δ 276.6 p.p.m. [*J*(PC) 48 Hz], and there are two CO peaks (211.1 and 205.5 p.p.m.). The two cage CMe groups are chemically non-equivalent and so there are two peaks for the *C*Me and the C*Me* groups in the spectrum. The asymmetry in the structure also leads to four MeP signals. There are correspondingly four resonances for the MeP groups in the ^{1}H n.m.r. spectrum.

It was apparent from the n.m.r. data for complex (**10a**) that it was an isomer of (**10b**), but with a more symmetrical structure. This would result if the B–Pt σ bond involved the boron atom in the CBCB*B*B ring which is not linked to a carbon atom, this isomer being defined for purposes of discussion as the β isomer. In the ^{13}C-{^{1}H} n.m.r. spectrum of (**10a**) (Table 1) there is only one CO resonance, in contrast with the two such signals observed in the spectrum of (**10b**). The cage CMe group in (**10a**) gives rise to two peaks (*C*Me and C*Me*) compared with the four such signals seen for this group in the spectrum of (**10b**). In the ^{1}H and ^{13}C-{^{1}H} n.m.r. spectra of (**10a**) there are two MeP group signals, as opposed to four such resonances in the spectra of (**10b**). These data for (**10a**) imply a plane of symmetry through the P, W, and Pt atoms and the boron atoms CBCB*B*B of the ring. An alternative structure for (**10a**) where the B–Pt σ bond involves the boron atom between the two carbons in the C*B*CBBB ring cannot be entirely eliminated. Such a structure would also have chemically equivalent CMe and CO groups in agreement with the ^{1}H and ^{13}C-{^{1}H} n.m.r. data. However, this possibility seems unlikely since the CMe groups would be less favourably disposed with respect to the PMe$_2$Ph ligands.

Formation of the complexes (**10**) from the reaction between (**6**) and $[\text{PtMe(thf)(PMe}_2\text{Ph)}_2][\text{BF}_4]$ implies a loss of CH_4, as in the synthesis of the compounds (**7**). The two reactions probably proceed by similar pathways with intermediates having both PtMe groups and B–H$\rightharpoonup$Pt bonds. The work described herein, as well as that described previously,[2] shows that a variety of tungsten–platinum complexes with unprecedented structures may be obtained *via* the salts (**1**) or (**6**).

Experimental

Light petroleum refers to that fraction of b.p. 40—60 °C, and all solvents were freshly distilled over appropriate drying agents prior to use. Chromatography columns (*ca.* 3 × 30 cm) were of alumina (Brockman, activity II), and all compounds were handled under oxygen-free nitrogen using Schlenk-tube techniques. The instrumentation used for the spectroscopic measurements has been described previously.[12] The reagent (**1c**) was prepared by the method used earlier to obtain the salt $[\text{NEt}_4][\text{W}(\equiv\text{CPh})(\text{CO})_2(\eta^5\text{-C}_2\text{B}_9\text{H}_9\text{Me}_2)]$ [13] and compound (**6**) was prepared as described previously.[11] The complex $[\text{PtCl(Me)(PMe}_2\text{Ph)}_2]$ was synthesised by treating *cis*-$[\text{PtMe}_2(\text{PMe}_2\text{Ph})_2]$ with HCl or MeCOCl. The former procedure affords the *cis* isomer of the platinum compound, and the latter the *trans* isomer. Either isomer can be used in the syntheses described below, in which $[\text{PtMe(Me}_2\text{CO)(PMe}_2\text{Ph)}_2][\text{BF}_4]$ is presumably generated *in situ*.[3]

Synthesis of the Tungsten–Platinum Complexes.—(*i*) A mixture of the compounds $[\text{PtCl(Me)(PMe}_2\text{Ph)}_2]$ (0.10 g, 0.20 mmol), TlBF_4 (0.06 g, 0.24 mmol), and (**1c**) (0.12 g, 0.20 mmol) was stirred in acetone (25 cm^3) for 1 h. The suspension was filtered through a Celite pad (*ca.* 2 cm), and solvent was removed *in vacuo* from the filtrate. The residue was dissolved in CH_2Cl_2–light petroleum (10 cm^3, 2:3) and chromatographed. Elution with the same solvent mixture gave two separable purple fractions. Removal of solvent *in vacuo* from the first eluate gave deep purple *microcrystals* of $[\text{WPt}(\mu\text{-CC}_6\text{H}_4\text{Me-4})(\mu\text{-}\sigma{:}\eta^5\text{-C}_2\text{B}_9\text{H}_8\text{Me}_2)(\text{CO})_2(\text{PMe}_2\text{Ph})_2]$ (**7a**) (β isomer) (0.05 g, 25%) (Found: C, 35.5; H, 4.4. $\text{C}_{30}\text{H}_{43}\text{B}_9\text{O}_2\text{P}_2\text{PtW}{\cdot}\text{CH}_2\text{Cl}_2$ requires C, 35.2; H, 4.2%); $\nu_{\text{max.}}$(CO) at 1 976m and 1 902m cm^{-1} (CH_2Cl_2). The second eluate, after removal of solvent *in vacuo*, yielded purple *microcrystals* of $[\text{WPt}(\mu\text{-CC}_6\text{H}_4\text{Me-4})(\mu\text{-}\sigma{:}\eta^5\text{-C}_2\text{B}_9\text{H}_8\text{Me}_2)(\text{CO})_2(\text{PMe}_2\text{Ph})_2]$ (**7b**) (α isomer) (0.09 g, 45%) (Found: C, 34.9; H, 4.4. $\text{C}_{30}\text{H}_{43}\text{B}_9\text{O}_2\text{P}_2\text{PtW}{\cdot}\text{CH}_2\text{Cl}_2$ requires C, 35.2; H, 4.2%); $\nu_{\text{max.}}$(CO) at 1 985m and 1 905m cm^{-1} (CH_2Cl_2).

Further elution of the chromatography column with CH_2Cl_2–light petroleum (4:1) gave a slow-running red fraction, which after removal of solvent *in vacuo* afforded the red oily salt $[\text{PtMe(PMe}_2\text{Ph)}_3][\text{W}_2\text{Pt}(\mu\text{-CC}_6\text{H}_4\text{Me-4})_2(\mu\text{-}\sigma{:}\eta^5\text{-C}_2\text{B}_9\text{H}_8\text{Me}_2)(\text{CO})_4(\eta^5\text{-C}_2\text{B}_9\text{H}_9\text{Me}_2)]$ (**8**) (0.01 g, 6%); $\nu_{\text{max.}}$(CO) at 1 986m, 1 970m, 1 916m, and 1 841w cm^{-1} (CH_2Cl_2). This product could not be crystallised, and its formulation is based on n.m.r. data (see text, and Table 1).

(*ii*) A mixture of the compounds $[\text{PtCl(Me)(PMe}_2\text{Ph)}_2]$ (0.05 g, 0.10 mmol), TlBF_4 (0.03 g, 0.12 mmol), and (**6**) (0.06 g, 0.10 mmol) in thf (20 cm^3) was stirred for 1 h. The resulting suspension was filtered through a Celite pad (*ca.* 1 cm), and solvent was removed *in vacuo*. The residue was dissolved in CH_2Cl_2–light petroleum (5 cm^3, 2:3) and chromatographed. Elution with the same solvent mixture gave a fast-running orange fraction, followed by a slower-running orange eluate. After removal of solvent *in vacuo* from the first fraction, orange *microcrystals* of $[\text{WPt}(\mu\text{-CC}_6\text{H}_4\text{Me-4})(\mu\text{-}\sigma{:}\eta^6\text{-C}_2\text{B}_{10}\text{H}_9\text{Me}_2)(\text{CO})_2(\text{PMe}_2\text{Ph})_2]$ (**10a**) (β isomer) (0.01 g, 14%) were obtained (Found: C, 35.1; H, 4.7. $\text{C}_{30}\text{H}_{44}\text{B}_{10}\text{O}_2\text{P}_2\text{PtW}{\cdot}\text{CH}_2\text{Cl}_2$ requires C, 34.8; H, 4.3%); $\nu_{\text{max.}}$(CO) at 2 007m and 1 956m cm^{-1} (CH_2Cl_2). The second eluate gave, after removal of solvent *in vacuo*, orange *microcrystals* of $[\text{WPt}(\mu\text{-CC}_6\text{H}_4\text{Me-4})(\mu\text{-}\sigma{:}\eta^6\text{-C}_2\text{B}_{10}\text{H}_9\text{Me}_2)(\text{CO})_2(\text{PMe}_2\text{Ph})_2]$ (**10b**) (α isomer) (0.06 g, 70%) (Found: C, 35.1; H, 4.5. $\text{C}_{30}\text{H}_{44}\text{B}_{10}\text{O}_2\text{P}_2\text{PtW}{\cdot}\text{CH}_2\text{Cl}_2$ requires C, 34.8; H, 4.3%); $\nu_{\text{max.}}$(CO) at 2 008m and 1 950m cm^{-1}.

Crystal Structure Determinations.—(*i*) Crystals of (**7a**) were grown as purple plates by diffusion of light petroleum into a CH_2Cl_2 solution of the complex at *ca.* −30 °C. Compound (**7a**) crystallised with one molecule of CH_2Cl_2 in the asymmetric unit. A crystal of suitable dimensions (*ca.* 0.30 × 0.20 × 0.10 mm) was sealed under nitrogen in a Lindemann tube, and diffracted intensities were measured (θ—2θ scans) at 298 K in the range $4 \leqslant 2\theta \leqslant 50°$ on a Nicolet *P*3 four-circle diffractometer. Of 6 864 unique data, 4 044 had $F \geqslant 6\sigma(F)$, and only these were used in the solution and refinement of the structure, after corrections for Lorentz, polarisation, and *X*-ray absorption effects. The latter correction was based on a semiempirical method using azimuthal scan data.[14]

Crystal data. $\text{C}_{30}\text{H}_{43}\text{B}_9\text{O}_2\text{P}_2\text{PtW}{\cdot}\text{CH}_2\text{Cl}_2$, $M = 1\,058.7$, monoclinic, space group $P2_1/c$ (no. 14), $a = 13.399(5)$, $b = 25.196(6)$, $c = 12.319(2)$ Å, $\beta = 110.73(2)°$, $U = 3\,889(2)$ Å^3, $Z = 4$, $D_c = 1.81$ g cm^{-3}, $F(000)$ 2 032, Mo-K_α *X*-radiation (graphite monochromator), $\bar{\lambda} = 0.710\,69$ Å, μ(Mo-K_α) = 69.0 cm^{-1}.

The structure of (**7a**) was solved by conventional heavy-atom methods, and successive difference Fourier syntheses were used to locate all non-hydrogen atoms, which were refined with anisotropic thermal parameters. All hydrogen atoms were included at calculated positions (C–H 0.96, B–H 1.10 Å)[15] with fixed isotropic thermal parameters (*ca.* 1.2 $U_{\text{equiv.}}$ of the parent carbon or boron atom). Refinement by blocked-cascade least squares led to $R = 0.042$ ($R' = 0.040$), and a weighting scheme of the form $w^{-1} = [\sigma^2(F) + 0.0005|F|^2]$ gave a satisfactory analysis of variance. The final electron-density difference synthesis showed no peaks $\geqslant 1.47$ or $\leqslant -0.93$ e Å^{-3}.

(*ii*) Crystals of (**10b**) were grown as orange prisms by diffusion

Table 5. Atomic positional parameters (fractional co-ordinates × 10^4) for compound (**7a**) with estimated standard deviations in parentheses

Atom	*x*	*y*	*z*	Atom	*x*	*y*	*z*
Pt	2 610(1)	1 536(1)	1 363(1)	C(8)	1 727(10)	889(5)	−1 017(11)
W	4 165(1)	1 104(1)	700(1)	C(9)	884(10)	1 236(5)	−1 512(11)
P(1)	2 287(3)	2 220(1)	2 394(3)	C(10)	18(11)	1 102(5)	−2 481(12)
P(2)	1 199(3)	999(1)	1 471(3)	C(11)	−43(11)	609(5)	−3 000(11)
Cl(1)	7 256(8)	1 224(4)	7 569(9)	C(12)	809(12)	267(6)	−2 526(12)
Cl(2)	5 796(8)	505(4)	6 031(8)	C(13)	1 675(11)	404(5)	−1 566(12)
O(5)	3 996(9)	898(5)	−1 873(10)	C(14)	−1 002(12)	462(6)	−4 050(13)
O(6)	4 081(11)	−120(5)	1 156(13)	C(15)	2 646(11)	2 151(5)	3 941(10)
B(3)	4 856(12)	1 966(6)	816(13)	C(16)	2 806(11)	2 878(5)	2 270(12)
B(4)	4 264(10)	1 779(6)	1 881(13)	C(17)	863(10)	2 377(4)	1 848(11)
B(5)	5 068(13)	1 253(6)	2 706(15)	C(18)	219(10)	2 381(5)	2 504(11)
B(6)	5 260(14)	1 925(7)	3 262(16)	C(19)	−813(12)	2 524(6)	2 055(13)
B(7)	5 114(13)	2 361(6)	2 072(16)	C(20)	−1 257(12)	2 667(6)	914(14)
B(8)	6 130(12)	2 195(6)	1 532(17)	C(21)	−645(11)	2 677(7)	240(14)
B(9)	6 898(13)	1 688(7)	2 407(18)	C(22)	438(12)	2 528(7)	705(13)
B(10)	6 349(13)	1 509(7)	3 431(16)	C(23)	1 303(13)	301(5)	1 144(14)
B(11)	6 385(14)	2 175(7)	3 015(18)	C(24)	−220(10)	1 107(7)	723(13)
C(1)	6 033(11)	1 156(6)	2 172(13)	C(25)	1 371(12)	961(5)	3 000(13)
C(2)	5 917(10)	1 537(5)	1 085(13)	C(26)	2 374(13)	799(6)	3 772(15)
C(3)	6 565(12)	607(6)	2 235(15)	C(27)	2 556(15)	780(7)	4 964(16)
C(4)	6 400(13)	1 386(7)	163(15)	C(28)	1 780(20)	922(7)	5 378(17)
C(5)	4 104(11)	957(6)	−916(13)	C(29)	820(16)	1 078(7)	4 643(17)
C(6)	4 122(11)	332(6)	973(13)	C(30)	603(12)	1 104(5)	3 440(13)
C(7)	2 667(10)	1 055(4)	−48(10)	C(31)	5 964(21)	1 114(9)	6 564(26)

Table 6. Atomic positional parameters (fractional co-ordinates × 10^4) for compound (**10b**) with estimated standard deviations in parentheses

Atom	*x*	*y*	*z*	Atom	*x*	*y*	*z*
Pt	7 235(1)	3 033(1)	6 822(1)	C(8)	6 985(8)	1 532(6)	5 809(6)
W	5 460(1)	2 344(1)	6 708(1)	C(9)	8 005(8)	1 379(6)	6 092(7)
P(1)	8 215(2)	3 909(2)	7 616(2)	C(10)	8 402(9)	846(7)	5 669(8)
P(2)	7 839(2)	3 209(2)	5 611(2)	C(11)	7 822(11)	491(7)	4 962(8)
Cl(1)	−363(3)	1 067(3)	8 382(3)	C(12)	6 821(10)	653(7)	4 697(8)
Cl(2)	971(5)	1 098(4)	7 328(4)	C(13)	6 417(8)	1 147(6)	5 125(7)
O(5)	4 966(7)	704(5)	6 279(6)	C(14)	8 313(12)	−69(8)	4 520(10)
O(6)	4 309(8)	2 825(6)	4 855(7)	C(15)	7 753(7)	4 821(6)	7 407(7)
B(3)	4 982(11)	1 902(8)	7 935(10)	C(16)	8 501(8)	3 875(8)	8 772(7)
B(4)	6 318(9)	3 101(7)	7 698(8)	C(17)	9 473(7)	3 900(6)	7 491(6)
B(5)	5 196(9)	3 560(7)	7 149(9)	C(18)	9 885(8)	4 512(7)	7 199(8)
B(6)	4 058(10)	3 081(8)	7 038(10)	C(19)	10 874(10)	4 471(10)	7 139(9)
B(7)	4 222(11)	2 765(9)	8 241(10)	C(20)	11 416(9)	3 858(11)	7 369(10)
B(8)	5 470(11)	2 427(8)	8 881(10)	C(21)	11 026(9)	3 284(10)	7 656(10)
B(9)	6 356(10)	3 022(8)	8 800(8)	C(22)	10 053(9)	3 309(7)	7 716(8)
B(10)	5 796(9)	3 792(8)	8 217(8)	C(23)	7 113(9)	2 827(7)	4 618(7)
B(11)	4 497(9)	3 678(8)	7 904(9)	C(24)	9 089(8)	2 988(7)	5 559(8)
B(12)	5 167(12)	3 334(9)	8 876(11)	C(25)	7 676(9)	4 156(7)	5 319(7)
C(1)	4 084(7)	2 253(7)	7 247(8)	C(26)	6 788(11)	4 463(8)	5 279(8)
C(2)	6 145(8)	2 301(6)	8 212(7)	C(27)	6 573(18)	5 142(10)	4 995(11)
C(3)	3 172(8)	1 808(7)	6 930(9)	C(28)	7 252(24)	5 555(12)	4 783(12)
C(4)	6 998(8)	1 730(7)	8 451(8)	C(29)	8 155(19)	5 292(11)	4 839(11)
C(5)	5 127(8)	1 293(7)	6 438(9)	C(30)	8 396(13)	4 576(8)	5 090(9)
C(6)	4 714(9)	2 618(7)	5 510(11)	C(31)	385(12)	581(9)	7 893(10)
C(7)	6 536(7)	2 065(5)	6 242(7)				

of light petroleum into a CH_2Cl_2 solution of the complex, which crystallised with one molecule of CH_2Cl_2 per asymmetric unit. A crystal of suitable dimensions (*ca.* 0.70 × 0.50 × 0.30 mm) was sealed in a Lindemann capillary tube, and diffracted intensities were collected as for (**7a**). Of the 4 904 unique data, 4 173 had $F \geqslant 6\sigma(F)$, and only these were used in the solution and refinement of the structure, after corrections for Lorentz, polarisation, and *X*-ray absorption.[14]

Crystal data. $C_{30}H_{44}B_{10}O_2P_2PtW{\cdot}CH_2Cl_2$, $M = 1\,070.5$, monoclinic, space group $P2_1/n$ (no. 14), $a = 13.930(5)$, $b = 18.57(1)$, $c = 16.331(6)$ Å, $\beta = 105.45(3)°$, $U = 4\,072(3)$ Å^3, $Z = 4$, $D_c = 1.75$ g cm^{-3}, $F(000)$ 1 892, μ(Mo-K_α) 65.1 cm^{-1}.

The structure was solved as for (**7a**). All hydrogen atoms were included at calculated positions with refined isotropic thermal parameters for hydrogens attached to boron atoms and fixed isotropic thermal parameters for those attached to the carbon atoms (*ca.* $1.2U_{\text{equiv.}}$ of the parent carbon atom). Refinement led to $R = 0.043$ ($R' = 0.044$), with a weighting scheme of the form $w^{-1} = [\sigma^2(F) + 0.0005|F|^2]$ giving a satisfactory analysis of variance. The final electron-density difference map showed no peaks $\geqslant 1.85$ or $\leqslant -1.89$ e Å^{-3}.

For both structures all calculations were performed on a DEC micro-Vax II computer with the SHELXTL PLUS system of programs.[14] Scattering factors with corrections for anomalous dispersion were taken from ref. 16. Atomic co-ordinates for **(7a)** and **(10b)** are listed in Tables 5 and 6, respectively.

Additional material available from the Cambridge Crystallographic Data Centre comprises H-atom co-ordinates, thermal parameters, and remaining bond distances and angles.

Acknowledgements

We thank the Spanish Consejo Superior de Investigaciones Científicas for a Fellowship (to M. C. G.) and the U.S.A.F. Office of Scientific Research (Grant 86-0125) for partial support.

References

1 Part 100, N. Carr, M. C. Gimeno, J. E. Goldberg, M. U. Pilotti, F. G. A. Stone, and I. Topaloğlu, *J. Chem. Soc., Dalton Trans.*, 1990, 2253.

2 (*a*) M. J. Attfield, J. A. K. Howard, A. N. de M. Jelfs, C. M. Nunn, and F. G. A. Stone, *J. Chem. Soc., Dalton Trans.*, 1987, 2219; (*b*) D. D. Devore, J. A. K. Howard, J. C. Jeffery, M. U. Pilotti, and F. G. A. Stone, *ibid.*, 1989, 303.

3 H. C. Clark and J. D. Ruddick, *Inorg. Chem.*, 1970, **9**, 1226.

4 E. O. Fischer, T. L. Lindner, G. Huttner, P. Friedrich, F. R. Kreissl, and J. O. Besenhard, *Chem. Ber.*, 1977, **110**, 3397.

5 O. Johnson, J. A. K. Howard, M. Kapan, and G. M. Reisner, *J. Chem. Soc., Dalton Trans.*, 1988, 2903.

6 J. A. Abad, L. W. Bateman, J. C. Jeffery, K. A. Mead, H. Razay, F. G. A. Stone, and P. Woodward, *J. Chem. Soc., Dalton Trans.*, 1983, 2075.

7 T. V. Ashworth, J. A. K. Howard, and F. G. A. Stone, *J. Chem. Soc., Dalton Trans.*, 1980, 1609.

8 J. A. Abad, E. Delgado, M. E. Garcia, M. J. Grosse-Ophoff, I. J. Hart, J. C. Jeffery, M. S. Simmons, and F. G. A. Stone, *J. Chem. Soc., Dalton Trans.*, 1987, 41; S. J. Davies and F. G. A. Stone, *ibid.*, 1989, 785.

9 P. S. Pregosin, R. Favez, R. Roulet, T. Boschi, R. A. Michelin, and R. Ros, *Inorg. Chim. Acta*, 1980, **45**, L7.

10 M. J. Chetcuti, K. Marsden, I. Moore, F. G. A. Stone, and P. Woodward, *J. Chem. Soc., Dalton Trans.*, 1982, 1749.

11 S. J. Crennell, D. D. Devore, S. J. B. Henderson, J. A. K. Howard, and F. G. A. Stone, *J. Chem. Soc., Dalton Trans.*, 1989, 1363.

12 S. J. Davies, J. A. K. Howard, M. U. Pilotti, and F. G. A. Stone, *J. Chem. Soc., Dalton Trans.*, 1989, 2289.

13 F-E. Baumann, J. A. K. Howard, O. Johnson, and F. G. A. Stone, *J. Chem. Soc., Dalton Trans.*, 1987, 2661.

14 G. M. Sheldrick, SHELXTL PLUS programs used with the Nicolet *X*-ray system.

15 P. Sherwood, BHGEN, a program for the calculation of idealised H positions for *nido*-icosahedral carbaborane fragments, Bristol University, 1986.

16 'International Tables for *X*-Ray Crystallography,' Kynoch Press, Birmingham, 1974, vol. 4.

Received 1*st February* 1990; *Paper* 0/00485E